

Designing for Robustness in Electric Grids via a General Effective Resistance Measure

Shriya V. Nagpal ^{*}, Gokul G. Nair, Francesca Parise [†], and C. Lindsay Anderson [†], *Senior Member, IEEE*

Abstract—We propose a mathematical framework for designing robust networks of coupled phase-oscillators by leveraging a vulnerability measure proposed by Tyloo et. al that quantifies how much a small perturbation to a phase-oscillator’s natural frequency impacts the system’s global synchronized frequencies. Given a fixed complex network topology with specific governing dynamics, the proposed framework finds an optimal allocation of edge weights that minimizes such vulnerability measure(s) at the node(s) for which we expect perturbations to occur by solving a tractable semidefinite programming problem. We specify the mathematical model to high voltage electric grids where each node corresponds to a voltage phase angle associated with a bus and edges correspond to transmission lines. Edge weights are determined by the susceptance values along the transmission lines. In this application, frequency synchronization is increasingly challenged by the integration of renewable energy, yet is imperative to the grid’s health and functionality. Our framework helps to alleviate this challenge by optimizing the placement of renewable generation and the susceptance values along the transmission lines.

Index Terms—Coupled phase-oscillators, convex optimization, frequency synchronization, high voltage electric grid, robust network design, renewable energy, semidefinite programming

I. INTRODUCTION

COMPLEX networks are frequently used to model coupled dynamical systems ranging from interacting molecules in chemical reactions [1] to high voltage electric grids [2]. Be it man-made or natural, elements of a coupled dynamical system are represented by nodes in a complex network, and two nodes are adjacent to one another if the differential equations that govern those nodes, are dependent on one another [2]. Two questions that are often investigated in complex networks are:

- 1) What are the vulnerable nodes of the complex network?
- 2) How can one use this knowledge to design robust complex networks?

^{*} indicates the corresponding author and [†] indicates equal contribution.

S. V. Nagpal and G. G. Nair are with the Center for Applied Mathematics, Cornell University, Ithaca, NY 14853 USA (e-mail: svn23@cornell.edu; gn234@cornell.edu).

F. Parise is with the School of Electrical and Computer Engineering and the Center for Applied Mathematics, Cornell University, Ithaca, NY 14853 USA (e-mail: fp264@cornell.edu).

C. L. Anderson is with the Department of Biological and Environmental Engineering and the Center for Applied Mathematics, Cornell University, Ithaca, NY 14853 USA (e-mail: cla28@cornell.edu).

In this work, we seek to address the latter question for a complex network of coupled phase-oscillators. Specifically, we consider a weighted, connected, and undirected network, $G = (V, E)$, where V is a set of n nodes and E is a set of m edges. $B \in \mathbb{R}^{n \times n}$ is the weighted adjacency matrix specifying the edge weights of G ; $B_{ij} = b_{ij} > 0$ if $(i, j) \in E$ and $B_{ij} = 0$ if $(i, j) \notin E$. Each node $i \in V$ in the network corresponds to an angle, $\theta_i \in [-\pi, \pi)$, that evolves according to the coupled dynamics

$$\dot{\theta}_i = \omega_i - \sum_j b_{ij} \sin(\theta_i - \theta_j), i = 1, \dots, n. \quad (1)$$

The phase-oscillator’s dynamics of node i is determined by its natural frequency, ω_i , and its coupling with other phase-oscillators determined by the network’s edge weights B . Despite the apparent simplicity, the coupled phase-oscillator model and its variations have been utilized to describe and analyze a broad array of applications including circadian rhythms, flashing fireflies, and high voltage electric grids [3]. In many of these phenomena, it is desirable for phase-oscillators to maintain global synchronized frequencies, i.e., $\theta_i = \omega_0$ for all $i \in \{1, \dots, n\}$.

Following [4], we measure vulnerability of a network by quantifying how much a small perturbation to a node’s/phase-oscillator’s natural frequency impacts the system’s global synchronized frequencies. A small external perturbation at a node with high vulnerability has a larger influence on the global synchronized frequencies than nodes with a smaller vulnerability measure. Interestingly, in [4] the author’s show that such a vulnerability measure may be written as a linear combination of effective resistance measures. In the remaining of this section, we recap intuition into the derivation of this measure and then describe how to leverage this vulnerability measure for the purpose of designing robust systems.

We apply the design framework to high voltage grids where each node i corresponds to a voltage phase angle $\theta_i \in [-\pi, \pi)$, associated with a bus i , and evolves according to the coupled dynamics given in (1), [5]–[7]. Here, the voltage phase-oscillators’ ability to maintain synchronized frequencies is essential to the functionality of the grid. The current administration plans to have wind and solar energy comprise ninety percent of the United State’s electricity profile by 2050 [8], but this integration will likely result in small perturbations to the power injected into the system, challenging the voltage phase-oscillators’ capacity to maintain synchronized frequencies. This work seeks to address this tension by optimizing

the placement of renewable generation and the susceptance values along the transmission lines to minimize the effect of disturbances on the voltage phase-oscillators' frequencies, in line with the proposed 2 billion dollar government investment for clean energy infrastructure [9].

A. Vulnerability Measure

Let $\omega^{(0)} = [\omega_1^{(0)}, \dots, \omega_n^{(0)}]^T$ be a vector of natural frequencies. When natural frequencies, $\omega_i^{(0)}$ for all i , are not too large compared to their coupling parameters, stable solutions exist where phase-oscillators have global synchronized frequencies, i.e., $\dot{\theta}_i = \omega_0$ for all $i \in \{1, \dots, n\}$ ¹ [10]. By working in a rotating reference frame, one may assume $\theta_i = 0$ for all i , resulting in a stable fixed point, $\theta^{(0)} = (\theta_1^{(0)}, \dots, \theta_n^{(0)})$. Subjecting $\omega_i^{(0)}$ to a time dependent perturbation, $\omega_i(t) = \omega_i^{(0)} + \tilde{\omega}_i(t)$, results in phase angles becoming time-dependent, $\theta_i(t) = \theta_i^{(0)} + \tilde{\theta}_i(t)$, and linearizing the dynamics around $\theta^{(0)}$ ultimately yields:

$$\dot{\tilde{\theta}}_i = \tilde{\omega}_i - \sum_j b_{ij} \cos(\theta_i^{(0)} - \theta_j^{(0)}) (\tilde{\theta}_i - \tilde{\theta}_j), i = 1, \dots, n. \quad (2)$$

Suppose k is some node in the network. To determine the vulnerability measure of this node we set $\tilde{\omega}_k(t)$ to a time dependent, Ornstein-Uhlenbeck noise disturbance, and $\tilde{\omega}_s = 0$ for all $s \neq k$. Let $\tilde{\theta}_i^{(k)}$ be a corresponding solution of (2).² We then define

$$\mathcal{M}(k) = \lim_{T \rightarrow \infty} T^{-1} \sum_i \int_0^T \left| \dot{\tilde{\theta}}_i^{(k)}(t) - \dot{\Delta}^{(k)}(t) \right|^2 dt \quad (3)$$

where $\dot{\Delta}^{(k)}(t) = n^{-1} \sum_j \dot{\tilde{\theta}}_j^{(k)}(t)$. Intuitively, this measure quantifies how much a specific perturbation at a node k impacts the global angular-frequency synchronization; If the measure is small, the oscillators' frequencies remain synchronized, or at least close in value, throughout time when exposed to a small perturbation.³ While (3) depends on the solution of an ordinary differential equation, in [4] it is shown that $\mathcal{M}(k)$ can be expressed in terms of network properties only. Specifically, in [4], the authors' derive an analytical expression for (3) and show that if the timescale of correlation in the noise is large in comparison to the dynamical system timescale, then

$$\mathcal{M}(k) = c_1 \left(n^{-1} \sum_j \Omega_{jk}(\theta^{(0)}, b) - n^{-2} \sum_{i < j} \Omega_{ij}(\theta^{(0)}, b) \right) \quad (4)$$

where c_1 is a fixed positive constant independent of the network, b is a m length vector that consists of all b_{ij} where $(i, j) \in E$, and

$$\Omega_{ij}(\theta^{(0)}, b) = \mathbb{L}_{ii}^\dagger(\theta^{(0)}) + \mathbb{L}_{jj}^\dagger(\theta^{(0)}) - 2\mathbb{L}_{ij}^\dagger(\theta^{(0)})$$

¹This statement is made more precise later on in this write up.

²We note that the Ornstein-Uhlenbeck process can be considered as the continuous-time analogue of the discrete-time $AR(1)$ process.

³The authors in [4] do make an implicit assumption that the perturbation is small enough such that the dynamics remain within the basin of attraction.

is the effective resistance [4] corresponding to the weighted network Laplacian matrix evaluated at a steady state, whose entries are given by

$$\mathbb{L}_{ij}(\theta^{(0)}) = -b_{ij} \cos(\theta_i^{(0)} - \theta_j^{(0)})$$

if $i \neq j$ and

$$\mathbb{L}_{ii}(\theta^{(0)}) = \sum_k b_{ik} \cos(\theta_i^{(0)} - \theta_k^{(0)}).$$

The same vulnerability measure may be derived by exposing oscillator k 's natural frequency to a temporary box noise perturbation, expanding the types of perturbations for which the vulnerability measure accounts for [10].

B. Existing Literature and Contributions

Various topological vulnerability measures have been discussed in the literature that quantify the ability of *identical* oscillators (i.e. $\omega_i^{(0)} = \bar{\omega}$ for all i) to maintain synchronized frequencies in the presence of small perturbations [10]–[12]. One such topological measure that has received considerable attention is the eigenratio of the network laplacian, $Q = \lambda_n/\lambda_2$, where $0 = \lambda_1 < \lambda_2 \leq \dots \leq \lambda_n$. Using the master stability framework proposed in Pecora et. al [13], it was shown that the interval in which the synchronized state is stable is larger for smaller Q [12]. Following this work, many papers have leveraged this measure for the purpose of exploring and designing robust systems governed by (1) [12]–[15].

However, many of these design frameworks are rendered incompatible with existing applications because many applications involve a network of *nonidentical* coupled oscillators, like high voltage electric grids. In this work, we consider *nonidentical* coupled oscillator networks and seek to *design* robust oscillator networks capable of maintaining global synchronized frequencies in the presence of noise by considering the vulnerability measure (4). In particular, we develop a mathematical framework for finding an optimal allocation of edge weights to minimize the vulnerability measure(s) at the node(s) for which we expect perturbations to occur subject to a fixed total amount of edge weight and a constraint that ensures synchronized frequencies, described in [16]. Under a small phase angle assumption, we show that the vulnerability measure considered in this work (4) is convex with respect to the edge weights of the network which implies that any edge assignment that results from the optimization framework is a global minimizer. We also provide a tractable semidefinite programming reformulation of the framework, and illustrate its utility by studying optimal placement of renewable energy.

The rest of the paper is divided as follows: In section 2 we develop the proposed optimization framework in detail, providing a proof of convexity of the vulnerability measure and a semidefinite programming (SDP) formulation of the optimization problem. In section 3, we apply the mathematical model developed in section 2 to the high voltage electric grid, and consider how the model may be used to inform the design of a grid that is robust to the integration of renewable energy. Finally, in section 4 we summarize the findings and propose some ideas for future exploration.

II. MATHEMATICAL MODEL

Given a fixed complex network topology with governing dynamics described by (1), this work's objective is to find an optimal allocation of edge weights to minimize the vulnerability measure at a node, or a function of vulnerability measures corresponding to a subset of nodes, for which we expect small perturbations to occur, subject to two constraints; The edge weights are non-negative and sum to 1.⁴ Specifically, the nodes for which we expect perturbations to occur is described by the subset $V' \subseteq V$, and in the application of interest, corresponds to busses where renewable energy is introduced. Edge weights correspond to susceptance values along the transmission lines and this work investigates how the distribution of susceptance values along the transmission lines of a high voltage electric grid topology facilitates robustness of that network.

To start, we work under the assumption that the difference between phase angles of a steady state, $|\theta_i^{(0)} - \theta_j^{(0)}|$, is small for all $(i, j) \in E$ implying that $\cos(\theta_i^{(0)} - \theta_j^{(0)}) \approx 1$.⁵ This means that for each $k \in V'$, $\mathcal{M}(k) \approx \mathcal{M}'(k) := n^{-1} \sum_j \Omega_{jk}(b) - n^{-2} \sum_{i < j} \Omega_{ij}(b)$ where $\Omega_{ij}(b) = \mathbb{L}_{ii}^\dagger + \mathbb{L}_{jj}^\dagger - 2\mathbb{L}_{ij}^\dagger$ is the effective resistance corresponding to the network laplacian, $\mathbb{L}_{ij} = -b_{ij}$ if $i \neq j$, and $\mathbb{L}_{ii} = \sum_k b_{ik}$. Suppose $V' = \{k^1, \dots, k^l\}$ where $l \leq n$. We wish to find $b^* \in \mathbb{R}^m$ to minimize a function of the vulnerability measures of nodes in V' , that is

$$b^* = \arg \min_b \mathcal{F}(\mathcal{M}'(k^1), \dots, \mathcal{M}'(k^l)) \quad (5)$$

s.t. $b \geq 0, \mathbf{1}^T b = 1$.

We choose $\mathcal{F}(\mathcal{M}'(k^1), \dots, \mathcal{M}'(k^l)) = \max_{k \in V'} \mathcal{M}'(k)$ to produce edge weights that optimally minimize the worst case vulnerability measure of nodes in V' . However, we emphasize that this framework allows for flexibility in the choice of \mathcal{F} depending on the desired definition of robustness in the application of interest. In the paragraphs that follow, we show that $\mathcal{M}'(k)$ is convex with respect to b , provide sufficient conditions for (5) to be convex in b for generic \mathcal{F} , and then show how to reformulate problem (5) (specified to this work's choice of \mathcal{F}) as a semidefinite programming (SDP) problem in order to employ efficient solvers.

A. Proof of Convexity

Theorem 1: Suppose $G = (V, E)$ is a simple, connected graph with $|V| = n$ and $|E| = m$. Let $b_{ij} \geq 0$ be the edge weight that corresponds to edge $(i, j) \in E$ and suppose b is a m length vector that consists of all b_{ij} . For each node $k \in V$, the measure $\mathcal{M}'(k)$ is convex with respect to the edge weights b .

Proof: Since \mathbb{L} is a real symmetric matrix, it can be written as $\mathbb{L} = V\Lambda V^T$ where $V \in \mathbb{R}^{n \times n}$, $\Lambda \in \mathbb{R}^{n \times n}$ are such that:

⁴This assumption is made for simplicity, but in reality, the edge weights may sum to any positive constant.

⁵Note that in the power grid, fixed points of the system are sought such that $|\theta_i^{(0)} - \theta_j^{(0)}|$ are small for all $(i, j) \in E$.

- $V^T V = V V^T = I$
- $\Lambda = \begin{bmatrix} \lambda_1 & 0 & \dots & 0 \\ 0 & \lambda_2 & \dots & 0 \\ \vdots & 0 & \ddots & 0 \\ 0 & \dots & 0 & \lambda_n \end{bmatrix}$

where $0 = \lambda_1 < \lambda_2 \leq \lambda_3 \dots \leq \lambda_n, \lambda_i \in \text{spec}(\mathbb{L})$. Moreover, the Moore–Penrose pseudoinverse of \mathbb{L} may be written as $\mathbb{L}^\dagger = (\mathbb{L} + \mathbf{1}\mathbf{1}^T/n)^{-1} - \mathbf{1}\mathbf{1}^T/n$ [17], or $\mathbb{L}^\dagger = V\Lambda^\dagger V^T$, for

$$\Lambda^\dagger = \begin{bmatrix} 0 & 0 & \dots & 0 \\ 0 & \frac{1}{\lambda_2} & \dots & 0 \\ \vdots & 0 & \ddots & 0 \\ 0 & \dots & 0 & \frac{1}{\lambda_n} \end{bmatrix}.$$

Now, for fixed k , consider the measure $\mathcal{M}'(k) = n^{-1} \sum_j \Omega_{jk}(b) - n^{-2} \sum_{i < j} \Omega_{ij}(b)$. Recall that e_k is a standard basis vector of length n , and let v_α denote the eigenvector associated with α^{th} eigenvalue of \mathbb{L} , i.e, the α^{th} column of V . Then,

$$\begin{aligned} \mathcal{M}'(k) &= n^{-1} \sum_j \Omega_{jk}(b) - n^{-2} \sum_{i < j} \Omega_{ij}(b) \\ &\stackrel{*}{=} \left(\sum_{\alpha \geq 2} \frac{v_{\alpha k}^2}{\lambda_\alpha} + n^{-2} \sum_{i < j} \Omega_{ij}(b) \right) - n^{-2} \sum_{i < j} \Omega_{ij}(b) \\ &= \sum_{\alpha \geq 2} \frac{v_{\alpha k}^2}{\lambda_\alpha} = \mathbb{L}_{kk}^\dagger = e_k^T \mathbb{L}^\dagger e_k \\ &= e_k^T (\mathbb{L} + \mathbf{1}\mathbf{1}^T/n)^{-1} - \mathbf{1}\mathbf{1}^T/n e_k \\ &= e_k^T (\mathbb{L} + \mathbf{1}\mathbf{1}^T/n)^{-1} e_k - e_k^T (\mathbf{1}\mathbf{1}^T/n) e_k \\ &= e_k^T (\mathbb{L} + \mathbf{1}\mathbf{1}^T/n)^{-1} e_k - \frac{1}{n}. \end{aligned}$$

For an explanation of the first equality (denoted with $*$) we refer the reader to the appendix. From [17], we observe that $f(Y) = c^T Y^{-1} c$, where $Y = Y^T \in \mathbb{R}^{n \times n}$ and $c \in \mathbb{R}^n$, is a convex function of Y for $Y \succ 0$. Consequently, since $(\mathbb{L} + \mathbf{1}\mathbf{1}^T/n)^{-1} \succ 0$ [17] and $\mathbb{L} + \mathbf{1}\mathbf{1}^T/n$ is an affine function of the edge weights of the graph G , $e_k^T (\mathbb{L} + \mathbf{1}\mathbf{1}^T/n)^{-1} e_k$ is a convex function of the edge weights of the graph. This means that $e_k^T (\mathbb{L} + \mathbf{1}\mathbf{1}^T/n)^{-1} e_k - \frac{1}{n}$ is a convex function of the edge weights of the graph since $\frac{1}{n}$ is simply a constant. ■

Corollary 1.1: If $\mathcal{F} : \mathbb{R}^{|V'|} \rightarrow \mathbb{R}$ is convex and nondecreasing, then $\mathcal{F}(\mathcal{M}'(k^1), \dots, \mathcal{M}'(k^l))$ is convex with respect to b .

Corollary 1.1 is proven in [18] and implies that $\max_{k \in V'} \mathcal{M}'(k)$ is convex with respect to the edge weights of b [17].

B. SDP Formulation

We now show how to reformulate problem (5) (specified to this work's choice of \mathcal{F}) into a SDP problem so that efficient solvers may be employed. By Theorem 1, (5) (specified to this work's choice of \mathcal{F}) may be written as:

$$\begin{aligned} \arg \min_b \max_{k \in V'} e_k^T (\mathbb{I} + \mathbf{1}\mathbf{1}^T/n)^{-1} e_k \\ \text{s.t. } b \geq 0 \text{ and } \mathbf{1}^T b = 1. \end{aligned} \quad (6)$$

Set a slack variable t such that

$$e_k^T (\mathbb{I} + \mathbf{1}\mathbf{1}^T/n)^{-1} e_k \leq t \text{ for all } k \in V'.$$

By Schur's complement, $e_k^T (\mathbb{I} + \mathbf{1}\mathbf{1}^T/n)^{-1} e_k \leq t$ for all $k \in V'$ if and only if

$$S_k := \begin{bmatrix} \mathbb{I} + \mathbf{1}\mathbf{1}^T/n & e_k \\ e_k^T & t \end{bmatrix} \succeq 0 \text{ for all } k.$$

Hence, problem (6), may be written as

$$\begin{aligned} \arg \min_b t \\ \text{s.t. } b \geq 0, \mathbf{1}^T b = 1, \\ S_k \succeq 0 \forall k \in V'. \end{aligned}$$

Construct the block diagonal matrix $Z \in \mathbb{R}^{d \times d}$ where $d = n(n+1) + m$ as:

$$Z = \begin{bmatrix} S_1 & & & & & & \\ & S_2 & & & & & \\ & & \ddots & & & & \\ & & & S_n & & & \\ & & & & b_1 & & \\ & & & & & b_2 & \\ & & & & & & \ddots \\ & & & & & & & b_m \end{bmatrix}.$$

Define $W \in \mathbb{R}^{d \times d}$ such that $W_{ij} = 1$ if and only if $i = j = n+1$, and $W_{ij} = 0$ otherwise. Define $A \in \mathbb{R}^{d \times d}$ such that $A_{ij} = 1$ if and only if

$$i \in \{(n+1)n+1, \dots, (n+1)n+m\}$$

and $i = j$, and $A_{ij} = 0$ otherwise. Then, coalescing everything together, results in the following SDP formulation of problem (6):

$$\begin{aligned} \arg \min_b \text{Tr}(WZ) \\ \text{s.t. } \text{Tr}(AZ) = 1, \\ Z \succeq 0. \end{aligned} \quad (7)$$

To solve (7) for b^* , we utilize CVXPY, a Python-embedded modeling language for convex optimization problems [19].

C. Graph Theoretic Interpretation

To shed light on the results attained from the optimization framework, (6), we analyze the vulnerability measure, $\mathcal{M}'(k)$, from a graph theoretic perspective. Let D be the weighted degree matrix of G and define a discrete-time transition probability matrix $P = D^{-1}B$. Such a transition probability matrix defines a random walk on the weighted graph G in

which a random walker at node i has probability P_{ij} of visiting node j in the next time step. The *expected hitting time*, H_{ij} , is the expected number of steps such a random walker takes to reach node j for the first time, starting from node i . The *expected commute time* is the expected number of steps a random walker takes to reach node j , starting at node i , and then return to node i ; $C_{ij} = H_{ij} + H_{ji}$ [20]. The following well-known result relates expected commute times and effective resistance [17]:

$$C_{ij} = 2(\mathbf{1}^T b) \Omega_{ij}(b) = 2\Omega_{ij}(b)$$

since $\mathbf{1}^T b = 1$. By multiplying both sides of

$$\mathcal{M}'(k) = n^{-1} \sum_j \Omega_{jk}(b) - n^{-2} \sum_{i < j} \Omega_{ij}(b)$$

by n^2 and recalling the definition of $\mathcal{M}'(k)$, we have

$$n^2 \mathcal{M}'(k) = \frac{1}{2}(n-1) \sum_j C_{jk} - \frac{1}{2} \sum_{\substack{i < j \\ i, j \neq k}} C_{ij}.$$

Thus, $2n^2 \mathcal{M}'(k) = (n-1) \sum_j C_{jk} - \sum_{i < j, i, j \neq k} C_{ij}$ and so minimizing the vulnerability measure $\mathcal{M}'(k)$ at a node k amounts to a trade-off among: (1) minimizing the expected commute time from node k to any other node in the system, and (2) maximizing the expected commute time between any two nodes in the system that are not k .

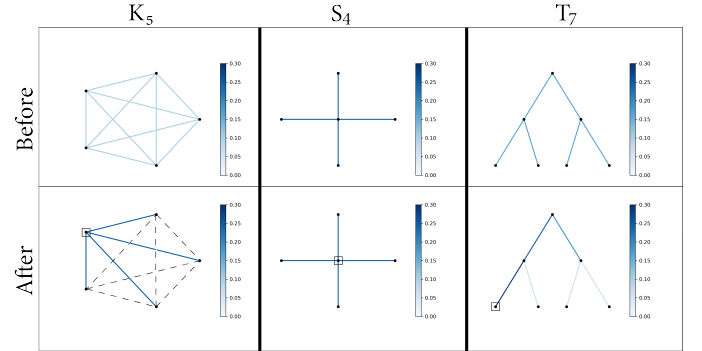


Fig. 1. We consider a complete graph (K_5), a star graph (S_4), and a tree (T_7). Each graph in the top row has the same edge weight for each edge such that all edges sum to one, and in the bottom row, we apply this optimization framework to exactly one node, node k , in the graph indicated by the black square. The vulnerability measure at each node, k , after the optimization framework either decreases or stays the same. If edges are dotted, this means that the edge weight is 0 at that edge.

Figure 1 demonstrates that in some cases both (1) and (2) can be achieved simultaneously, while in others, this is a nontrivial trade-off. Specifically, in the scenario (K_5) the sum of the expected commute time from node k to any other node in the system decreases and the sum of the expected commute time between any two nodes in the system that are not k increases. This is the best scenario for minimizing $\mathcal{M}'(k)$. In (S_4), the edge weights, and therefore commute times, do

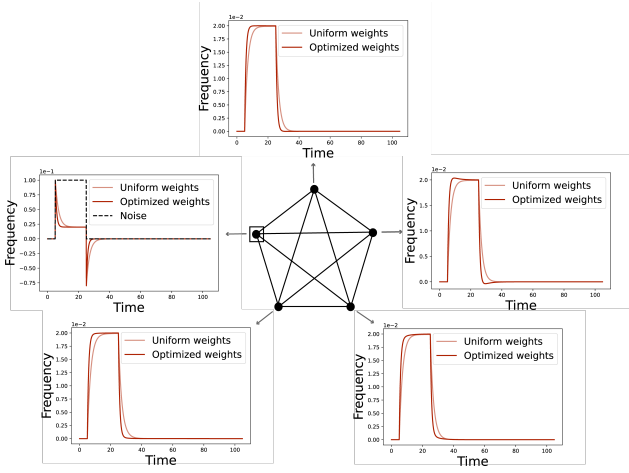


Fig. 2. The node that is squared on the complete graph on five nodes in the center of this image is the node with perturbed natural frequency for both the uniform edge weight case and optimized edge weight case. Each node on the graph has an associated arrow which points to a plot where the oscillators' frequencies over time for both cases, uniform and optimized edge weights, are considered. For each of these plots, we consider time (seconds) on the x -axis and frequency (in a co-rotating frame) on the y -axis.

not change. In (T_7) , the sum of expected commute time from node k to any other node in the system decreases, but, as a consequence, the sum of the expected commute time between any two nodes in the system that are not k decreases. This is a nontrivial trade-off.

To give insight on how assigning edge weights such that this graph theoretic/commute time interpretation is satisfied permits a system of oscillators' whose synchronized frequencies are robust to perturbations via simulation we consider a complete graph on five nodes with uniform edge weights and synchronized frequencies and expose a specific oscillator's/node's natural frequency to a temporary box noise perturbation. Then, we consider the same complete graph on five nodes with edge weights obtained from the optimization framework and synchronized frequencies and expose the same node's natural frequency to the same temporary box noise perturbation. For both cases, we plot in Figure 2 the oscillators' frequencies over time for the purpose of comparison.

It is interesting to note that for all five nodes, the oscillators' frequencies behavior in the uniform edge weight case and optimized edge weights case are qualitatively similar except for one caveat; The oscillators frequencies' behavior in the uniform edge weights case seems to slightly lag the oscillators frequencies' behavior in the optimized edge weights case. We observe this qualitative behavior when performing the same type of simulation on T_7 and a figure elucidating this can be seen in the appendix section.

This nicely connects the graph theoretic interpretation to the vulnerability measure (3) definition.⁶ In assigning edge weights such that the commute time interpretation is satisfied we are permitting perturbations introduced at node k to have more of an influence and, therefore, propagate to other nodes

⁶Here, recall that vulnerability measure (3) is derived in [10] for box noise perturbations.

at a quicker speed. This allows for oscillators' frequencies to synchronize at a quicker rate, or at least remain close in value, throughout time when a node is exposed to a small perturbation. We observe this same qualitative behavior when node k 's natural frequency is exposed to an Ornstein-Uhlenbeck noise disturbance, however, the box noise perturbation lends itself to a sharper illustration.

D. Ensuring Synchronicity

In the derivation of the vulnerability measure, we assumed that the oscillators have synchronized frequencies and small phase angle differences. This assumption is not always true and is dependent on the relationship between the oscillators' natural frequencies and the edge weights of the complex network. The work [16] delineates a condition relating complex networks oscillators' natural frequencies and edge weights that ensures the existence of a stable synchronized solution with phase angle differences less than a given small angle parameter, γ . Specifically, the authors show that if the second smallest eigenvalue, $\lambda_2(b)$ of \mathbb{L} satisfies

$$\lambda_2(b) \geq \sin(\gamma) \|H(b)\omega^0\|_\infty, \quad (8)$$

then $|\theta_i^{(0)} - \theta_j^{(0)}| \leq \gamma$ for a wide class of networks. Here, $\|\cdot\|_\infty$ is the maximum norm and $H(b) \in \mathbb{R}^{2m \times n}$ is the incidence matrix of the network G thought of as a directed graph (by replacing each edge by two directed edges going in opposite directions) and is defined component-wise as $H_{kl} = 1$ ($H_{kl} = -1$) if node l is the sink (source) of edge k and zero otherwise.

Thus, to ensure that a synchronized stable solution with angle difference less than a chosen, small angle parameter γ exists, we incorporate (8) as a constraint into the optimization framework. Note that (8) is not convex in b . In order to accommodate such a constraint into the SDP formulation and maintain tractability, we use a procedure inspired by the scenario approach. To this end, note that since $\mathbf{1}$ is the first eigenvector of \mathbb{L} , we can write

$$\lambda_2(b) = \min_{\substack{\|x\|_2=1 \\ \mathbf{1}^T x=0}} x^T \mathbb{L} x. \quad (9)$$

The condition, $\mathbf{1}^T x = 0$ ensures that we are minimizing over the orthogonal complement of $\mathbf{1}$, the first eigenvector. Thus we can rewrite the constraint (8) as

$$x^T \mathbb{L} x \geq \sin(\gamma) \|H(b)\omega^0\|_\infty \text{ for all } x \perp \mathbf{1}, \|x\|_2 = 1. \quad (10)$$

(10) is a continuous collection of infinitely many constraints. For tractability, we pick a finite number, N of them corresponding to a set $\{x_1, \dots, x_N\}$ chosen uniformly at random and approximate (10) with the following N inequalities,

$$x_i^T \mathbb{L} x_i \geq \sin(\gamma) \|H(b)\omega^0\|_\infty \quad i = 1, \dots, N. \quad (11)$$

The rest of this paper considers the optimization framework to be (6) subject to the N additional constraints described in (11), and b^* to be the solution to this optimization framework. We choose the number N following the *scenario approach* [21] and treat x as if it were a random variable

uniformly distributed on the set $\Upsilon = \{x \in \mathbb{R}^n : \|x\|_2 = 1, \mathbf{1}^T x = 0\}$. To be more precise, we choose *confidence* and *violation* parameters $\beta, \epsilon \in (0, 1)$ and pick N uniformly distributed points on Υ with $N \geq \frac{2}{\epsilon} \left(\ln \frac{1}{\beta} + m \right)$. If x were indeed a random variable, this choice would guarantee that b^* would satisfy the constraint (10) for all $x \perp \mathbf{1}$ and $\|x\|_2 = 1$ but at most an ϵ -fraction with probability no smaller than $1 - \beta$, i.e. $\text{Prob}(x : x^T \mathbb{L} x \not\geq \sin(\gamma) \|H(b)\omega^0\|_\infty) \leq \epsilon$, where Prob is the uniform probability measure on Υ .

III. HIGH VOLTAGE ELECTRIC GRID APPLICATION

An electrical grid is an interconnected network, consisting of transmission lines and busses, designed for the purpose of delivering power from producers to consumers. Power is delivered from generator busses to load busses via the transmission lines by way of alternating current, depicted by a sinusoidal curve. Electrical impedance is the measure of opposition that a transmission line presents to alternating current when a voltage is applied. Specifically, in the power grid, impedance of transmission lines are comprised of resistance and reactance. Busses where power is generated are called generator busses and have net positive power injections into the system whereas busses where power is consumed are called load busses and have net negative power injections into the system because power is being consumed at these locations.

Suppose we are considering a high voltage electric grid consisting of n busses and m transmission lines. We may model the grid as a connected network, $G = (V, E)$, with n nodes and m edges where each node $i \in V$ corresponds to a voltage phase angle $\theta_i \in [-\pi, \pi)$, associated with a bus i , and evolves according to the coupled dynamics [5]–[7] described in (1) where ω_i is the per unit power injected at node i , and $\sum_{j=1}^N b_{ij} \sin(\theta_i - \theta_j)$ is the per unit power extracted at node i .⁷ We note that b_{ij} is the per unit susceptance along the transmission line that connects bus i to bus j . Concretely, b_{ij} is calculated by taking the reciprocal of the per unit reactance along the transmission line that connects bus i to bus j in the physical system, and intuitively describes how conductive the transmission line is.

As previously stated, the ability for voltage phase-oscillators participating in the system to maintain frequency synchronization is imperative to the health and functionality of the electric grid, and this ability is potentially threatened by the integration of renewable energy into the high voltage electric grid. Indeed, with the integration of renewable energy we expect to see small perturbations to the power injected into the system at certain busses. Thus, we leverage the model as a design tool for ensuring the grid is robust to the integration of renewable energy. We consider two scenarios whose solutions amount to ensuring that a fixed amount of susceptance⁸ is optimally allocated to the edges of a fixed power grid topology to minimize the vulnerability measure at nodes where renewable energy is introduced.

⁷Note that there would be a damping term that we assume to be 1 second for now.

⁸Normalized to one, for simplicity, and informed by a fixed amount of physical resources.

A. Data set Description

We consider a 57 bus case system that is a high voltage electric grid model for the NY region [22]. The dataset consists of 29 generator busses, 28 load busses, and 94 transmission lines. To establish a natural frequency corresponding to each voltage phase-oscillator participating in the system, we attain the per unit power injected information associated with each node during a cold morning in December 2020. For all of the problem scenarios considered, following the discussion in Section II, we ensure synchronicity by setting $\beta = \epsilon = 0.01$, and correspondingly choose $N = 1054$. Lastly, we set $\gamma = \frac{\pi}{16}$.

B. Scenario 1

Suppose a power grid engineer is tasked with converting the energy source at a generator bus to a renewable energy source which will likely result in small perturbations to the power injected at that bus. Is there a generator bus that would be the most robust to the introduction of renewable energy? Does the choice of bus change given the ability to distribute a fixed amount of susceptance to the edges of the electric grid network?

To address this scenario with the proposed mathematical framework, we find optimal allocations of susceptance values, b_k^* , for each of the k nodes corresponding to the twenty-nine generator busses in the system, that minimize $\mathcal{M}'(k)$ subject to previously discussed constraints. For each of these nodes, k , we calculate $\mathcal{M}'(k)$ using the original susceptance values attained from data and compare this to $\mathcal{M}'(k)$ calculated via b_k^* . In all twenty-nine cases, the $\mathcal{M}'(k)$ calculated using the original susceptance values is greater than $\mathcal{M}'(k)$ calculated using b_k^* . Comparing $\mathcal{M}'(k)$ for each node k calculated by using b_k^* , the generator bus indexed as node 8 exhibits the smallest vulnerability measure and the generator bus indexed as node 12 exhibits the largest vulnerability measure after applying the optimization framework.

Since the generator bus indexed as node 8 exhibits the smallest vulnerability measure after applying the optimization framework, this bus would be the most robust to the introduction of renewable energy given the ability to distribute a fixed amount of susceptance to the edges of the electric grid network. Note that the generator bus exhibiting the smallest vulnerability measure in the network prior to optimization (indexed as node 15) is 54.6% larger than the vulnerability measure generator bus indexed as node 8 exhibits in the optimized network with weights b_k^* .

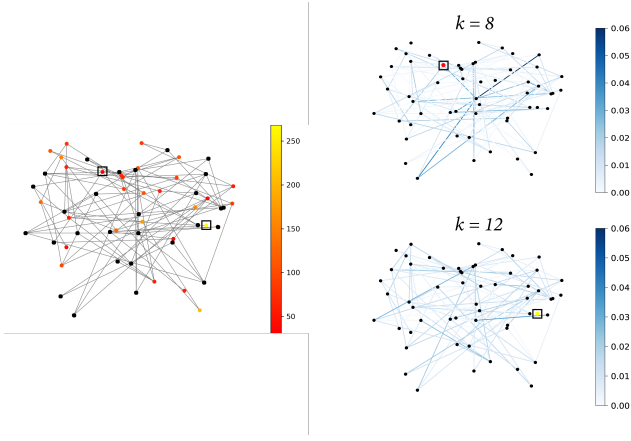


Fig. 3. All three graphs plot the 57 bus case system. In the left most graph, black nodes represent load busses and colored nodes represent generator busses. Each node corresponding to a generator bus, k , is colored according to its vulnerability measure, $\mathcal{M}'(k)$, in the optimized network with weights b_k^* . Notably, $\mathcal{M}'(8) \approx 30.85$ and $\mathcal{M}'(12) \approx 268.25$. Nodes 8 and 12 are highlighted via a black square. The two graphs on the right have edge weights that correspond to b_8^* and b_{12}^* highlighted by the blue color bars.

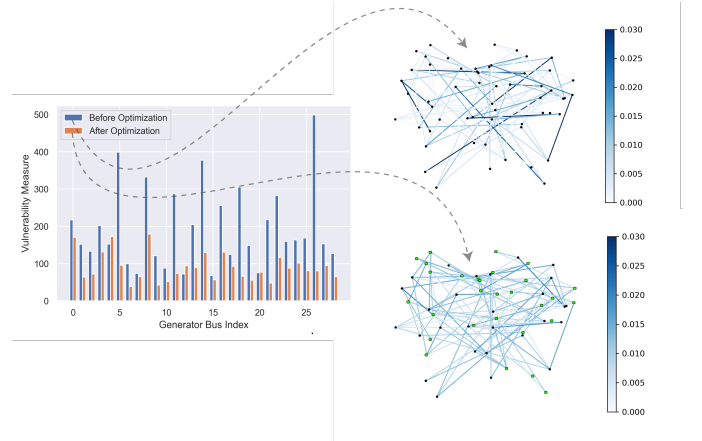


Fig. 4. In the left most plot, we consider the $\mathcal{M}'(k)$ for each $k \in V'$ before and after the optimization framework. The top most graph on the right has edge weights that correspond to the original susceptance values determined by data, and the bottom most graph on the right has edge weights that correspond to solving the optimization framework when V' is the set of generator nodes. The generator nodes are indicated by the color green in this graph.

C. Scenario 2

Generating power using renewable energy resources rather than fossil fuels reduces greenhouse gas emissions, and thus, helps address climate change [23]. Incorporating renewable energy at all the generator busses in the system will, however, likely result in small perturbations to the power injection at all these nodes. Can we distribute a fixed amount of susceptance to the edges of the electric grid network in such a way that allows for the voltage phase-oscillators' synchronized frequencies to be robust to noise at any of the generator busses?

This problem amounts to solving the proposed mathematical framework where V' is the set of nodes corresponding to generator busses in the complex network. Before applying the optimization framework, $\sum_{k \in V'} \mathcal{M}'(k) \approx 5663.14$, and after, $\sum_{k \in V'} \mathcal{M}'(k) \approx 2628.66$, amounting to approximately a 53.6% decrease in the total vulnerability measure at the generator nodes in the complex network after applying the optimization framework. As illustrated by the plot in Figure 4, the vulnerability measure at each bus $k \in V'$ decreases after the optimization framework except for three generator busses indexed as node 4, 12, and 20. In these cases, the vulnerability measure increases after applying the optimization framework by absolute values of approximately 20.17, 21.84, and 1.20, respectively.

IV. CONCLUSION

In this work, we considered a small angle variation of the vulnerability measure derived in [4] that quantifies how much a small perturbation to a phase-oscillator's natural frequency impacts the system's global synchronized frequencies. Given a fixed total amount of edge weight, we proposed a mathematical framework that assigns an optimal allocation of edge weights to minimize the vulnerability measure at node k , $\mathcal{M}'(k)$, or a function of vulnerability measures corresponding to a subset of nodes V' , \mathcal{F} , for which we expect small perturbations to occur. The model allows for flexibility in the choice of \mathcal{F} contingent on the desired definition of robustness. In this work we specified \mathcal{F} to produce edge weights that optimally minimize the worst case vulnerability measure of nodes in V' , $\max_{k \in V'} \mathcal{M}'(k)$.

We proved that the vulnerability measure considered in this work is convex with respect to the edge weights of the network, implying that any edge weight assignment that results from the specified optimization problem is a global minimizer. Additionally, this work provided a tractable SDP reformulation of the problem and incorporated a constraint that ensures the existence of a synchronized stable solution with small angle difference via a procedure inspired by the scenario approach. Finally, we applied the framework to high voltage electric grids, addressing two scenarios that highlight how the mathematical model may be leveraged to alleviate tensions between current green initiatives and the high voltage electric grids' capacity to accommodate such initiatives.

There are many natural extensions to this work, both theoretical and applied in nature. One theoretical questions to investigate is whether the vulnerability measure considered in this work is strictly convex with respect to the edge weights of a graph. If this property holds, this would imply that the solution obtained from the mathematical framework is a unique global minimizer. On the other hand, recall that in establishing a natural frequency corresponding to each voltage phase-oscillator participating in the high voltage electric grid,

we attained the per unit power injected information associated with a specific time. In reality, the high voltage electric grid is a highly dynamic system where the power injected at each bus varies in time. Thus, it would be informative to analyze how (if at all) the susceptance values assigned along the transmission lines vary in reference to time-series power injection data. If the susceptance values assigned along the transmission lines vary in reference to time-series power injection data, one could further quantify the variance and construct structures that minimize the variance of assigned susceptance values.

APPENDIX I PROOF OF CONVEXITY CONTINUED

Lemma 2 ()*: Suppose $\mathbb{L} \in \mathbb{R}^{n \times n}$ is the network laplacian associated with simple, connected graph $G = (V, E)$, and let v_α be the eigenvector associated with the α^{th} eigenvalue of \mathbb{L} . Then,

$$n^{-1} \sum_j \Omega_{jk}(b) = \sum_{\alpha \geq 2} \frac{v_{\alpha k}^2}{\lambda_\alpha} + n^{-2} \sum_{i < j} \Omega_{ij}(b)$$

where $\Omega_{ij}(b) = \mathbb{L}_{ii}^\dagger + \mathbb{L}_{jj}^\dagger - 2\mathbb{L}_{ij}^\dagger$.

Proof: By equation (2) in [2], for a fixed node k we have:

$$\begin{aligned} n^{-1} \sum_j \Omega_{jk}(b) &= \frac{1}{n} \sum_{j=1}^n \sum_{\alpha \geq 2} \frac{(v_{\alpha j} - v_{\alpha k})^2}{\lambda_\alpha} \\ &= \frac{1}{n} \sum_{j=1}^n \sum_{\alpha \geq 2} \frac{v_{\alpha j}^2 - 2v_{\alpha j}v_{\alpha k} + v_{\alpha k}^2}{\lambda_\alpha} \\ &= \frac{1}{n} \sum_{j=1}^n \sum_{\alpha \geq 2} \frac{v_{\alpha k}^2}{\lambda_\alpha} + \frac{1}{n} \sum_{j=1}^n \sum_{\alpha \geq 2} \frac{v_{\alpha j}^2}{\lambda_\alpha} - \mathcal{K} \\ &= \sum_{\alpha \geq 2} \frac{v_{\alpha k}^2}{\lambda_\alpha} + \frac{1}{n} \sum_{\alpha \geq 2} \sum_{j=1}^n \frac{v_{\alpha j}^2}{\lambda_\alpha} - \mathcal{K} \\ &\stackrel{a}{=} \sum_{\alpha \geq 2} \frac{v_{\alpha k}^2}{\lambda_\alpha} + \frac{1}{n} \sum_{\alpha \geq 2} \frac{1}{\lambda_\alpha} - \mathcal{K} \\ &= \sum_{\alpha \geq 2} \frac{v_{\alpha k}^2}{\lambda_\alpha} + \frac{1}{n} \sum_{\alpha \geq 2} \frac{1}{\lambda_\alpha} - \frac{1}{n} \sum_{\alpha \geq 2} \frac{2v_{\alpha k}}{\lambda_\alpha} \sum_{j=1}^n v_{\alpha j} \\ &= \sum_{\alpha \geq 2} \frac{v_{\alpha k}^2}{\lambda_\alpha} + \frac{1}{n} \sum_{\alpha \geq 2} \frac{1}{\lambda_\alpha} - \frac{1}{n} \sum_{\alpha \geq 2} \frac{2v_{\alpha k}}{\lambda_\alpha} (v_\alpha^T \mathbf{1}) \\ &\stackrel{b}{=} \sum_{\alpha \geq 2} \frac{v_{\alpha k}^2}{\lambda_\alpha} + \frac{1}{n} \sum_{\alpha \geq 2} \frac{1}{\lambda_\alpha} \\ &\stackrel{c}{=} \sum_{\alpha \geq 2} \frac{v_{\alpha k}^2}{\lambda_\alpha} + n^{-2} \sum_{i < j} \Omega_{ij}(b) \end{aligned}$$

where $\mathcal{K} = \frac{1}{n} \sum_{j=1}^n \sum_{\alpha \geq 2} \frac{2v_{\alpha j}v_{\alpha k}}{\lambda_\alpha}$ and $\stackrel{a}{=}$, $\stackrel{b}{=}$, and $\stackrel{c}{=}$ hold because of the orthonormal columns of V , $v_\alpha^T \mathbf{1} = 0$, and equation (4) in [2], respectively. ■

APPENDIX II SCENARIO APPROACH

As discussed in the main text, we use a scenario approach to accommodate constraint (10). To this end, we have to generate

N uniformly distributed points on $\{x \in \mathbb{R}^n : x \perp \mathbf{1}, \|x\|_2 = 1\} \equiv \mathbf{1}^\perp \cap \mathbb{S}^{n-1}$, where $\mathbf{1}^\perp$ denotes the hyperplane orthogonal to the vector $\mathbf{1}$ and \mathbb{S}^{n-1} represents the $(n-1)$ -dimensional unit sphere with centre at the origin. This is done using the following algorithm:

- 1) Sample X from an n -dimensional standard normal distribution:

$$X \sim \mathcal{N}_n(0, 1)$$

where $f_X = Ce^{-\frac{1}{2}X \cdot X}$ is the probability density function of the random variable X .⁹

- 2) Project X onto the hyperplane, $\mathbf{1}^\perp$ by subtracting the mean from each component:

$$Y := X - \frac{\sum_{i=1}^n X_i}{n} \mathbf{1}$$

- 3) Normalize Y :

$$R = \frac{Y}{\|Y\|_2}.$$

Almost surely, R will lie on the set of interest, $\mathbf{1}^\perp \cap \mathbb{S}^{n-1}$. Since the multivariate normal distribution is radially symmetric, the probability density depends only on the distance from the origin. Since every point in $\mathbf{1}^\perp \cap \mathbb{S}^{n-1}$ is equidistant from the origin, the random variable, Y is uniformly distributed on this set.

APPENDIX III GRAPH THEORETIC INTERPRETATION CONTINUED

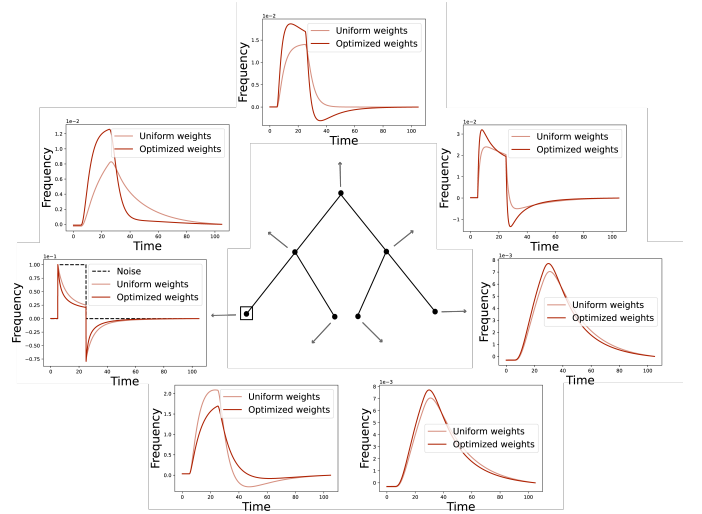


Fig. 5. The node that is squared on \mathcal{T}_7 in the center of this image is the node where we perturb the natural frequency for both the uniform edge weight case and optimized edge weight case. Each node on the graph has an associated arrow which points to a plot where the oscillators' frequencies over time for both cases, uniform and optimized edge weights are considered. For each of these plots, we consider time (seconds) on the x -axis and frequency (in a co-rotating frame) on the y -axis.

ACKNOWLEDGMENT

S. V. Nagpal and G. Nair would like to thank a few members from the Center for Applied Mathematics community

⁹ C is just the normalization constant.

at Cornell University for helpful conversations at varying stages in this work: Steve Strogatz, Maximilian Ruth, Shawn Ong, Misha Padidar, and Zachary Frangella. S. V. Nagpal and C. L. Anderson would like to acknowledge the Cornell Atkinson Center for Sustainability and the Cornell Energy Systems Institute funds for support. Finally, S. V. Nagpal would like to acknowledge the NSF Research Training Group Grant: Dynamics, Probability, and PDEs in Pure and Applied Mathematics, DMS-1645643 for partially funding this work.

REFERENCES

- [1] G. Filatrella, A. H. Nielsen, and N. F. Pedersen, "Analysis of a power grid using a kuramoto-like model," *The European Physical Journal B*, vol. 61, no. 4, pp. 485–491, 2008.
- [2] M. Tyloo and P. Jacquod, "Global robustness versus local vulnerabilities in complex synchronous networks," *Physical Review E*, vol. 100, no. 3, p. 032303, 2019.
- [3] F. Dörfler and F. Bullo, "Exploring synchronization in complex oscillator networks," in *2012 IEEE 51st IEEE Conference on Decision and Control (CDC)*. IEEE, 2012, pp. 7157–7170.
- [4] M. Tyloo, L. Pagnier, and P. Jacquod, "The key player problem in complex oscillator networks and electric power grids: Resistance centralities identify local vulnerabilities," *Science advances*, vol. 5, no. 11, p. eaaw8359, 2019.
- [5] Y. Guo, D. Zhang, Z. Li, Q. Wang, and D. Yu, "Overviews on the applications of the kuramoto model in modern power system analysis," *International Journal of Electrical Power & Energy Systems*, vol. 129, p. 106804, 2021.
- [6] S. Strogatz, *Sync: The emerging science of spontaneous order*. Penguin UK, 2004.
- [7] X. Hu, S. Boccaletti, W. Huang, X. Zhang, Z. Liu, S. Guan, and C.-H. Lai, "Exact solution for first-order synchronization transition in a generalized kuramoto model," *Scientific reports*, vol. 4, no. 1, pp. 1–6, 2014.
- [8] J. Engel, "Biden blueprint calls for wind and solar to power 90% of u.s. grid by 2050," *Renewable Energy World*, 2021. [Online]. Available: <https://www.renewableenergyworld.com/solar/biden-blueprint-calls-for-wind-and-solar-to-power-90-of-u-s-grid-by-2050/>
- [9] E. Penrod, "Biden proposes more than \$2b for clean energy infrastructure, \$14b+ increase in climate spending," *Utility Dive*, 2021. [Online]. Available: <https://www.utilitydive.com/news/biden-proposes-more-than-2b-for-clean-energy-infrastructure-14b-increase/>
- [10] M. Tyloo, T. Coletta, and P. Jacquod, "Robustness of synchrony in complex networks and generalized kirchhoff indices," *Physical review letters*, vol. 120, no. 8, p. 084101, 2018.
- [11] M. Fazlyab, F. Dörfler, and V. M. Preciado, "Optimal network design for synchronization of coupled oscillators," *Automatica*, vol. 84, pp. 181–189, 2017.
- [12] L. Donetti, P. I. Hurtado, and M. A. Muñoz, "Entangled networks, synchronization, and optimal network topology," *Phys. Rev. Lett.*, vol. 95, p. 188701, Oct 2005.
- [13] L. M. Pecora and T. L. Carroll, "Master stability functions for synchronized coupled systems," *Phys. Rev. Lett.*, vol. 80, pp. 2109–2112, Mar 1998.
- [14] L. Kempton, G. Herrmann, and M. d. Bernardo, "Self-organization of weighted networks for optimal synchronizability," *IEEE Transactions on Control of Network Systems*, vol. 5, no. 4, pp. 1541–1550, 2018.
- [15] H. Hong, B. J. Kim, M. Y. Choi, and H. Park, "Factors that predict better synchronizability on complex networks," *Phys. Rev. E*, vol. 69, p. 067105, Jun 2004.
- [16] F. Bullo, *Lectures on network systems*. Kindle Direct Publishing, 2019.
- [17] A. Ghosh, S. Boyd, and A. Saberi, "Minimizing effective resistance of a graph," *SIAM review*, vol. 50, no. 1, pp. 37–66, 2008.
- [18] S. Boyd and L. Vandenberghe, *Convex optimization*. Cambridge university press, 2004.
- [19] S. Diamond and S. Boyd, "Cvxpy: A python-embedded modeling language for convex optimization," *The Journal of Machine Learning Research*, vol. 17, no. 1, pp. 2909–2913, 2016.
- [20] P. Van Mieghem, K. Devriendt, and H. Cetinay, "Pseudoinverse of the laplacian and best spreader node in a network," *Physical Review E*, vol. 96, no. 3, p. 032311, 2017.
- [21] M. C. Campi, S. Garatti, and M. Prandini, "The scenario approach for systems and control design," *Annual Reviews in Control*, vol. 33, no. 2, pp. 149–157, 2009.
- [22] M. V. Liu, B. Yuan, Z. Wang, J. A. Sward, K. M. Zhang, and C. L. Anderson, "An open source representation for the nys electric grid to support power grid and market transition studies," 2021.
- [23] C. Nunez, "Renewable energy explained," *National Geographic*, 2020. [Online]. Available: <https://www.nationalgeographic.org/article/renewable-energy-explained/>